Resonator-Based Filter-Banks for Frequency-Domain Applications

Mukund Padmanabhan, *Student Member, IEEE*, and Ken Martin, *Fellow, IEEE*

Abstract—**Filter-bank structures have traditionally been used for several applications that require the decomposition of a signal into its main spectral components. The filter-bank structure proposed here is based on a digital simulation of a singly terminated ladder filter. This filter-bank can also be arrived at from a filter described earlier by Peceli, and represents an extremely hardware efficient structure, having a complexity of $O(N)$. The main application examined is adaptive line enhancement; the filter-bank-based line enhancer is shown to have the necessary conditions for global convergence, and to yield uncorrelated sinusoidal enhanced outputs that are undistorted versions of the corresponding frequency components of the input. A number of additional possible applications for the filter-bank are described; these include the tracking of periodic signals, sub-band coding, frequency-domain adaptive noise-cancellation, and frequency-domain processing of signals from phased arrays.**

I. Introduction

THE use of a filter-bank of IIR biquadratic filters for the spectral decomposition and analysis of signals has been popular for many years. Recently, a new filter-bank structure has received a good deal of attention. This structure has a complexity that is proportional to the number of bandpass outputs, and can have the filter resonant frequencies arbitrarily set. Further, the transfer functions from the input to the individual outputs are exactly unity at the resonant frequencies of the corresponding biquads and have transmission zeros at the frequencies of all the other biquads. The structure of the filter-bank consists of a number of undamped resonators with common feedback around all of them, as shown in Fig. 1.

This structure (with slight variations) can be independently arrived at by using three different approaches. The approach described in [1] and [2] is based on [9] and uses observer theory to estimate the states of a hypothetical system of resonators that model the input signal. The approach described in [3] and [4] is based on [7] and [8] and tries to match the weighted sum of oscillator outputs to the input signal using an LMS adaptive algorithm.

The approach described herein was based on a tone-decoder originally used in the telecommunications industry [6]. This tone-decoder was an active *RC* realization of the singly terminated ladder filter shown in Fig. 2(a).[1] The transfer function from the input current to the current through each resonator is exactly unity at the frequency of that resonator and has transmission zeros at the frequencies of all other resonators. A signal-flow-graph simulation of this filter is shown in Fig. 2(b). The structures described in this paper are based on replacing each continuous time integrator loop in Fig. 2(b) by an undamped digital biquad. In this paper, we primarily consider lossless discrete integrator (LDI) based biquads [25], which are known to be hardware efficient structures with good noise and sensitivity properties.

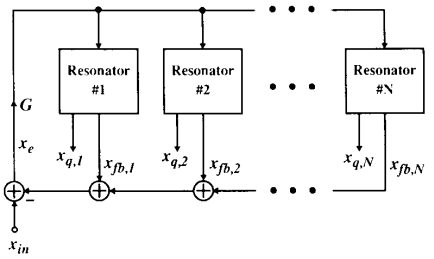

Fig. 1. Filter-bank structure.

The proposed filter-bank has a number of possible applications. It can be used in most applications where DFT's are presently being used for spectral analysis.[2] In addition, it can be used in applications where it is necessary to arbitrarily set the filter-bank resonant frequencies, as for tone decoding. It is even possible to adapt the resonant frequencies to track input signal components for spectral line enhancement. The filter-bank possesses the desired quality that the enhanced outputs have the same magnitude and phase as the input spectral components. It is shown that a straightforward approach to adapting the individual resonant frequencies does not result in global convergence, and is computationally intensive. A modified approach is proposed that possesses the necessary conditions for global convergence. Also, the modified

Manuscript received January 8, 1990; revised July 20, 1990. This work was supported in part by the National Science Foundation under Grant MIP-8913164. This paper was recommended by Associate Editor R. K. Hester.

The authors are with the Integrated Circuits and Systems Laboratory, University of California, Los Angeles, CA 90024.

IEEE Log Number 9102161.

[1] As was pointed out by one of the reviewers, Fig. 2(a) could also be interpreted as a singly terminated Cauer parallel realization of a lossless two port (obtained by using a partial fraction expansion of the admittance matrix of the lossless two port [32]).

[2] Though the filter has all real coefficients, it is possible to obtain complex outputs, which may be needed in some cases. The manner in which this can be done is described in Section 2.2.

0098-4094/91/1000-1145$01.00 ©1991 IEEE

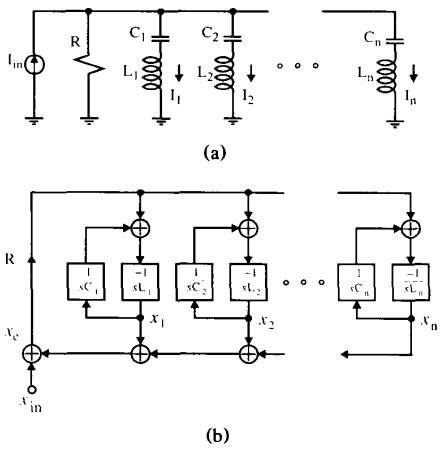

Fig. 2. (a) Singly terminated $L-C$ ladder. (b) Signal flow graph of singly terminated ladder filter.

approach is shown to yield an unbiased estimate of the frequency, when a single resonator is tracking a single input frequency in noise.

A number of other possible applications for the resonator-based filter-bank are also described. These include the tracking of periodic signals, sub-band coding, frequency-domain noise-cancellation and equalization, and the processing of multi-narrow-band signals from phased-array sensors.

Finally, a number of computer simulations of the adaptive filter-bank are described. Many of these are done with low SNR's and closely spaced sinusoids, sometimes with the sinusoids having very different powers.

II. Filter-Bank Structures with Uncorrelated Sinusoidal[3] Outputs

A digital realization of the signal-flow-graph of Fig. 2(b) can be obtained by replacing each resonator by an undamped digital biquad. Following switched-capacitor techniques [26], we will first consider the case where LDI-based biquads are used. The use of these biquads is also seen to provide an additional insight into the filter-bank structure. Subsequently, the filter-bank structure will be generalized so that any form of digital resonator may be used to replace the resonators of Fig. 1.

2.1. LDI-Based Filter-Bank

The LDI-based biquad is shown in Fig. 3(a) and corresponds to an undamped bandpass structure. If the signal feedback is taken from $x_{1,i}$, then the bandwidth of the

[3]If the input signal is the sum of as many sinusoids as there are second-order sections, and if their frequencies are the same as the resonator frequencies, then the bandpass outputs are sinusoidal and uncorrelated. However, if the damping factor G is chosen to be $1/2N$, and if the resonant frequencies are low, the bandpass outputs are also almost orthogonal in the strict sense, i.e., uncorrelated for white noise input.

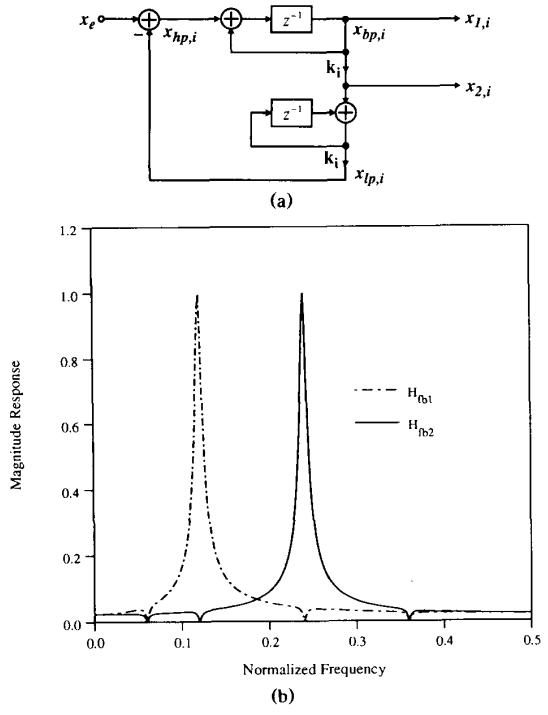

Fig. 3. (a) LDI based biquad. (b) Transfer function from filter-bank input to bandpass outputs.

bandpass outputs of the structure of Fig. 1 will be approximately independent of the internal biquad coefficients k_i. If $x_{2,i}$ is used as the common feedback term, then the Q-factor of the bandpass outputs is approximately independent of the internal k_i coefficients. The first case is appropriate if the bandpass outputs are to be evenly spaced in the frequency range, whereas the second case is more appropriate if the biquads are to be logarithmically placed throughout the frequency range of interest.

The transfer function from the input to the ith output ($x_{fb,i}$) of the filter-bank of Fig. 1 is given by

$$H_{bp,i}(z) = \frac{GH_i(z)}{1+G\sum_{j=1}^{N} H_j(z)} \tag{1}$$

where

$$H_i(z) = \frac{z^{-1}(1-z^{-1})}{1-(2-k_i^2)z^{-1}+z^{-2}}$$

$$\text{or} \quad \frac{k_i z^{-1}(1-z^{-1})}{1-(2-k_i^2)z^{-1}+z^{-2}} \tag{2}$$

depending on whether the common feedback term is taken from $x_{1,i}$ or $x_{2,i}$ of Fig. 3(a). The resonant frequency of each biquad is given by the equation

$$\omega_i T = 2\arcsin(k_i/2). \tag{3}$$

At this frequency, the transfer function $H_{bp,i}(z)$ will have

exactly unity gain; however, the maximum of the magnitude of $H_{bp,i}(z)$ can be larger than unity, and can occur at frequencies different from the resonant frequency. This is especially true for large G (low Q) and close spaced resonator frequencies.

By using the properties of "reactive" one-ports, it is possible to show that the transfer function from the input to the node labelled x_e in Fig. 2(b) is zero at the resonator frequencies and is exactly unity at some frequency between any two adjacent biquads. However, unlike the signal-flow-graph of the continuous-time circuit, the transfer function of the discrete realization from the input to the node x_e can have magnitude larger than unity due to the imperfect mapping of the LDI transform.

In order to ensure the stability of the overall structure, constraints need to be placed on the internal coefficients of the biquads (in this case k_i). For the single resonator case, the required condition is $0 \leqslant k_i \leqslant 2\sqrt{1-G}$. For the general Nth-order case, however, it is difficult to derive the constraints on the k_i, for which the filter remains stable. However, by slightly modifying the resonators, it becomes possible to relate the digital structure, through the bilinear transform, to a passive LCR circuit. It now becomes possible to derive constraints on the internal coefficients of the filter for which the filter is stable, by imposing the restriction that the L, C, and R of the associated analog circuit are non-negative (shown in the next section). This modification involves feeding back both the bandpass and low-pass outputs of the various resonators instead of the bandpass output alone. This digital filter structure can also be arrived at based on the results of [1] and [3] and will be described next.

2.2. *A Comparison to Other Approaches—The Generalized Resonator-Based Filter-Bank*

As mentioned in the introduction, other approaches to spectral estimation, starting from different points, have resulted in very similar structures. It was shown in [7] that the input signal could be matched to the weighted sum of reference oscillator outputs, the weights being updated by the LMS algorithm. Drawing on the analysis of [3] and [8] obtained the transfer function from the input to the ith weighted oscillator output, and the form of this transfer function was used to suggest the filter structure. The independent approach of [1] and [2] was based on [9], and started off with structures to obtain certain transforms of the given signal (such as the DFT). A state-space model for the signal was assumed, and an identity observer [9] was used to reconstruct the states of the model, from which the desired transforms of the signal were obtained. As the signal was modeled as the sum of the outputs of a bank of resonators, the identity observer turned out to have a "resonator-in-feedback-loop" structure, and the potentiality of this structure for general filtering applications was later realized and reported in [1].

In both of the above approaches, the resulting filter-bank consists of a number of first-order complex filters having transfer functions given by

$$H_i(z) = \frac{z_i z^{-1}}{1 - z_i z^{-1}} \tag{4}$$

where z_i are complex coefficients. Here, the first-order filters with complex conjugate poles can be combined and implemented by a single undamped biquad having the transfer function

$$H_{i,i^*}(z) = \frac{2z^{-1}(a_i - z^{-1})}{1 - 2a_i z^{-1} + z^{-2}} \tag{5}$$

where a_i is the real part of z_i and is given by $a_i = \cos(\omega_i T)$. We will now show that this structure can be arrived at by bilinear transforming an analog prototype of the form of Fig. 2(a).

At this stage, we are still free to choose any biquad structure to implement the transfer function (5). We will consider only biquads whose resonant frequencies are controlled by a single internal coefficient, henceforth to be referred to as k_i. This k_i will be related to a_i in a manner dependent on the biquad structure. Hence, for the LDI biquads,

$$k_i = \sqrt{2(1-a_i)} = 2\sin(\omega_i T/2). \tag{6}$$

The transfer function $H_e = x_e / x_{in}$ of Fig. 1, with a pair of complex conjugate $H_i(z)$ replaced by a $H_{i,i^*}(z)$ of the form (5), can be written as

$$H_e(z) = \frac{x_e}{x_{in}} = \frac{1}{1 + G\sum_{i=0}^{N-1} \dfrac{2a_i z^{-1} - 2z^{-2}}{1 - 2a_i z^{-1} + z^{-2}}} \tag{7}$$

$$= \frac{1}{1 - NG + G\sum_{i=0}^{N-1} \dfrac{1 - z^{-2}}{1 - 2a_i z^{-1} + z^{-2}}}. \tag{8}$$

Now, substituting $z = (1+s)/(1-s)$, we get an equivalent transfer function in the s domain, of the form

$$H_e(s) = \frac{1}{1 - NG + G\sum_{i=0}^{N-1} \dfrac{2s}{(1+a_i)s^2 + (1-a_i)}}. \tag{9}$$

If R in Fig. 2(a) is replaced by $1 - NG$, (9) may be seen to be related to the transfer function I_R / I_{in} of Fig. 2(a), through the scale factor $1/(1-NG)$, and the digital transfer function of (8) may be obtained by replacing all analog integrators $1/s$ in (9) by bilinear integrators

$(1+z^{-1})/(1-z^{-1})$. Since the bilinear transform maps poles in the left half of the s-plane to poles inside the unit circle of the z-plane, if (9) represents a stable transfer function, so does (8). In order to ensure that (9) is stable, we need to constrain all L, C, and R elements of Fig. 2(a) to be non-negative, which leads to the conditions[4]

$$G < \frac{1}{N} \quad \text{and} \quad -1 < a_i < 1. \tag{10}$$

The derived expressions and simulations in the following sections are with reference to the above filter-bank structure.

Fig. 3(b) shows a plot of the magnitude of the transfer functions $H_{fb,i}(z)$ for a four-resonator system, with G set equal to $1/12N$. Here, $H_{fb,i}(z)$ denotes the transfer function from the input of the filter-bank to the ith output $x_{fb,i}$ of Fig. 1, and is seen to have zeros at the frequencies of all other resonators, and exactly unit magnitude at the ith resonator frequency; hence the fed back signal is exactly in phase with the corresponding component in the input. Further, the transfer function from x_e to $x_{q,i}$ of Fig. 1 is given by

$$H_{q,i}(z) = \frac{2\sqrt{1-a_i}\,z^{-1}}{1-2a_i z^{-1}+z^{-2}}. \tag{11}$$

At the resonant frequency of the ith biquad, the transfer function $H_{q,i}(z)$ has identical amplitude and exactly $-90°$ phase shift when compared to the transfer function $H_{fb,i}(z)$. This quadrature or low-pass output will prove to be very useful in some of the applications that are described in later sections. This output corresponds to the difference of the outputs of a pair of first-order resonators having complex conjugate poles. As $x_{fb,i}$ represents the sum of the outputs of the above two resonators, $x_{fb,i} \pm jx_{q,i}$ represents the complex outputs of the first-order resonators; hence the structure may also be used in applications where the above complex outputs are required.

III. Adaptive Applications of the Resonator-Based Filter-Bank

3.1. Spectral Line Enhancement

One possible application of the filter-bank is to track the frequencies of the components of a multi-sinusoidal input signal by adapting the frequencies of the resonators in the filter-bank. As mentioned earlier, after convergence, this produces the isolated individual components at the feedback outputs. A previous adaptive line enhancer that could also be used for this application was reported in [10] and [11]. This structure was a cascade of notch biquads, and in order to adapt the notch frequencies, approximately $N^2/2$ biquads were required to produce the sensitivities of the error signal. The desire to reduce this complexity was one of the major motivations for the development of this filter-bank. Besides the reduced complexity, the filter-bank has the additional feature that the enhanced isolated outputs are *undistorted* versions of the input signal components unlike most other approaches, including the cascade line enhancer of [11].[5] It does have a disadvantage that for closely spaced sinusoids, after convergence, the transfer functions to the individual outputs can have magnitudes considerably greater than unity at frequencies between the input sinusoid frequencies; however, at the frequencies of the sinusoids, the gain is exactly unity.

In using the filter-bank to track sinusoids, the biquad resonant frequencies are adapted to minimize the signal x_e in Fig. 1. This minimization is achieved by adapting the coefficients until the correlation between the signal x_e and the outputs of certain "sensitivity" filters are all equal to zero. In most adaptive applications, the correlation between the ith sensitivity output and the error signal gives the gradient of the error power $E[x_e^2]$ with respect to the ith coefficient k_i, and the coefficient k_i is adapted in the direction opposite the gradient. As was shown in [10], the sensitivity filter for the ith coefficient usually has a transfer function given by

$$H_{s,i}(z) = \frac{dH_e(z)}{da_i}\frac{da_i}{dk_i} \tag{12}$$

where $H_e(z)$ is the transfer function from the input to the error. Here, k_i is the internal coefficient of the ith biquad, that determines its resonant frequency, and is related to the $a_i(=\cos(\omega_i T))$ in a manner that is dependent on the actual biquad structure used. We will only consider biquads that satisfy the constraints

i) The biquad resonant frequency is determined by the single coefficient k_i

ii) $\dfrac{da_i}{dk_i}$ has the same sign for all possible values of k_i (13)

(examples are LDI-based biquads, direct-form biquads, etc). The sensitivity filter for this case turns out to be equal to

$$H_{s,i}(z) = -2G\frac{da_i}{dk_i}A(z)A(z)z^{-1}(1-z^{-2}) \tag{14}$$

[4]A recent paper by McGee and Zhang [33] should be mentioned in this context, as similar ideas seem to have been used there.

[5]The ALE of [10] can be used with some slight modifications to recover an enhanced and undistorted signal, as shown in [13].

where

$$A(z)=\frac{\dfrac{1}{1-2a_iz^{-1}+z^{-2}}}{1+G\sum_{n=1}^{N}\dfrac{2a_iz^{-1}-2z^{-2}}{1-2a_iz^{-1}+z^{-2}}}. \quad (15)$$

The gradient of the error power with respect to the ith coefficient is generated by correlating the outputs of $H_{s,i}(z)$ and the error signal x_e.

Unfortunately, this approach has two problems. Firstly, the complexity of generating the outputs of the sensitivity filters is proportional to N^2, which is approximately twice that required by the cascade approach of [10] and [11]. More importantly, it will be shown that this approach does not have global convergence when N biquads are used to track N sinusoids ($N>1$) in the absence of noise. This comes about because the error power as a function of the resonator coefficients has several nonoptimal local minima; hence the true gradient cannot be used to update the coefficients.

For global convergence, the following requirements are necessary:[6]

i) For a negative da_i/dk_i the correlation between the ith sensitivity filter output and the error signal must be larger than or equal to zero for all input frequencies less than the resonant frequency of the corresponding biquad, and less than or equal to zero for all input frequencies larger than the corresponding resonant frequency. For a positive da_i/dk_i, the polarity of the correlation should be the opposite of the above.

ii) The correlation between the ith sensitivity filter output and the error signal must be equal to zero only when the input frequency is equal to the resonant frequency of any biquad.

It is assumed here that the number of resonators is equal to the number of sinusoids. Further, to prevent the tracking of two biquads from being identical, the update coefficients of the individual resonators are taken slightly different from each other. Also, by using an instantaneous estimate of the correlation between the sensitivity and the error for the update, it is ensured that the filter will not settle at unstable "saddle points."

As mentioned before, the gradient (denoted ∇_i) is given by the correlation of the error and the sensitivity output. Hence it may be written as

$$\nabla_i=\frac{1}{2\pi j}\oint H_e(z^{-1})H_{s,i}(z)X(z)X(z^{-1})z^{-1}dz \quad (16)$$

where $X(z)$ is the z-transform of the input signal. Assuming that the input is the sum of pure sinusoids, and that all but the ith biquad have converged to the corresponding input sinusoids, the output of the ith sensitivity filter will be a single sinusoid. If the frequency and input amplitude of this sinusoid are ω and A, respectively, then the gradient is given by

$$\nabla_i(\omega)=\frac{A^2}{2}\operatorname{Re}\{H_e^*(\omega)H_{s,i}(\omega)\}$$

$$=\frac{A^2}{2}\operatorname{Re}\{H_e(z^{-1})H_{s,i}(z)|_{z=e^{j\omega}}\}. \quad (17)$$

Writing $H_e(z^{-1})$ as $A(z^{-1})(1-2a_iz+z^2)$,

$$\nabla_i(\omega)=-2G\frac{da_i}{dk_i}\operatorname{Re}\{A(z)A(z^{-1})z^{-1}(1-2a_iz+z^2)\cdot(1-z^{-2})A(z)|_{z=e^{j\omega}}\} \quad (18)$$

$$=-2G\frac{da_i}{dk_i}\operatorname{Re}\{|A(\omega)|^2[2\cos(\omega)-2a_i]\cdot 2\sin(\omega)e^{j(\pi/2-\omega)}|A(\omega)|e^{j\phi(\omega)}\} \quad (19)$$

$$=2G\frac{da_i}{dk_i}|A(\omega)|^2[2a_i-2\cos(\omega)]\cdot 2\sin(\omega)\cos(\pi/2+\phi(\omega)-\omega)|A(\omega)| \quad (20)$$

where $A(z)|_{z=e^{j\omega}}=|A(\omega)|e^{j\phi(\omega)}$. Now, $|A(\omega)|$ is a positive quantity that has zeros at all resonator frequencies except the ith resonator frequency. Further, as $\cos(\omega_i)=a_i$, and as $\cos(\omega)$ is a monotonically decreasing function in $[0,\pi]$, we have

$$2a_i-2\cos(\omega)\begin{cases}<0, & \omega<\omega_i\\ >0, & \omega>\omega_i\\ =0, & \omega=\omega_i\end{cases}. \quad (21)$$

Under the assumptions (13), from (20), the first two terms in the expression for $\nabla_i(\omega)$ grouped together provide the properties that we would like the gradient to have. Further, the third term $\sin(\omega)$, is positive, for $\omega\in[0,\pi]$, and it is the cos( ) term in (20) that causes the gradient to lose the desired properties. $\phi(\omega)$ in this last term is given by

$$\phi(\omega)=\omega-\arctan\left[\frac{2G\sin(\omega)}{1-GN}K\right],\ \omega<\omega_i \quad (22)$$

$$=\omega-\arctan\left[\frac{2G\sin(\omega)}{1-GN}K\right]+\pi,\ \omega>\omega_i \quad (23)$$

where

$$K=\sum_{i=1}^{i=N}\frac{1}{2\cos(\omega)-2a_i}. \quad (24)$$

When $\cos(\pi/2-\omega+\phi(\omega))$ is evaluated, it is seen that the quantity becomes negative in regions between the resonant frequencies, implying that global convergence is not obtained. This is because of the nonconvexity of the error surface. To illustrate, a plot of the error power for a two-resonator system is shown in Fig. 4(a). The two input

[6]The necessary conditions are sufficient if all but a single biquad have converged to the frequencies of the corresponding input sinusoids. If more than one biquad has not converged, it is speculated that the conditions are sufficient, but this has not been proved. In all simulations of adapting N biquads to N sinusoids, global convergence was obtained in the absence of noise.

sinusoidal frequencies and the effective a_i of one of the resonators are fixed at 0.1, 0.0955, and 0.809, respectively, and the error power is shown as a function of the effective a_i of the other resonator. The corresponding gradients for the two resonators, with the effective a_i of the resonators, and one of the input frequencies fixed at 0.875, 0.809, and 0.1, respectively, is shown in Fig. 4(b), as a function of the other input frequency. It is seen that the gradient changes sign between the two resonator frequencies, and the necessary conditions for global convergences are not satisfied.

In the next section, a different filter is proposed for the "sensitivity" filter. This "pseudosensitivity" filter is much simpler to realize, and has the necessary conditions for global convergence. Furthermore, it will be shown that for the single resonator case, there is no bias in the presence of white noise.

3.1.1. The Pseudogradient: As was seen in the previous section, the generation of the true sensitivity is computationally intensive, and its use does not provide global convergence. In investigating alternatives for the true sensitivity filter, one possibility was found that did not have these deficiencies.[7]

In the proposed adaptive filter, the outputs of "pseudosensitivity" filters are correlated with the error output to give pseudogradients, which are then used to adapt the coefficients. The proposed "pseudosensitivity" filters have transfer functions equal to that from the filter-bank input to the low-pass or quadrature output of each resonator ($x_{q,i}$ of Fig. 1), multiplied by a scale factor.

Thus, in adapting the filter, one simply changes the ith coefficient to drive the correlation between the error signal and the ith low-pass output to zero. There is no additional complexity in generating the "pseudosensitivity" filter outputs; they can be obtained from the internal nodes of the filter-bank itself. The pseudosensitivity filters have transfer functions given by

$$H_{ps,i}(z) = -2G\frac{da_i}{dk_i}A(z)z^{-1} \tag{25}$$

and following the same procedure as for the true gradient, an expression can be developed for the pseudogradient analogous to (20) as

$$\nabla_i^{ps}(\omega) = -2G\frac{da_i}{dk_i}A^2(\omega)[2\cos(\omega) - 2a_i]. \tag{26}$$

Comparing (20) and (26), we see that the troublesome cos( ) term in (20) has been eliminated in (26). Hence the pseudogradient is easily shown to have the necessary conditions for global convergence, i.e., for positive (negative) da_i/dk_i

i) $\nabla_i^{ps}(\omega) < (>)\ 0$ if $\omega \leqslant \omega_i$ and $\nabla_i^{ps}(\omega) > (<)\ 0$ if $\omega > \omega_i$;

ii) $\nabla_i^{ps}(\omega) = 0\ \forall \omega = \omega_j$ where ω_j are the resonant frequencies given by (3).

As was pointed out by one of the reviewers, this particular pseudogradient appears to be very similar to the frequency update used in an earlier proposed method for frequency estimation [12]. However, the update used in this paper is felt to be more robust and less complicated than the method of [12].[8]

A plot of the pseudogradient for a two resonator system is shown in Fig. 5. After the resonators have converged to their steady states, the frequency of the input sinusoid may be obtained using the functional relationship between the coefficient k_i and the resonant frequency of the biquad ω_i. To avoid the computational overhead of evaluating this function, lookup tables may be used. A point worth noting is that the relation between k_i and ω_i is independent of the other k_j and also of G, the damping of the loop. Hence only one table of values need be maintained which is valid for all values of the damping.

3.1.2. Bias in the Resonator Frequency: In this section, it is shown that for the case of a single resonator tracking a single input sinusoid in additive white Gaussian noise, the resonator frequency converges to exactly the frequency of the input sinusoid without any bias. Assuming the input to be a sinusoid of frequency ω_{in} and amplitude A, and the noise to be additive white Gaussian with variance σ^2, the correlation between the pseudosensitivity output and the error output has an additional term due to the noise and now becomes

$$\nabla(\omega_{in}) = \nabla_1^{ps}(\omega_{res}, \omega_{in}) + \frac{2\sigma^2}{2\pi}\,\mathrm{Re}\left\{\int_0^{\pi} H_e^*(\omega)H_{ps,1}(\omega)\,d\omega\right\}$$

where $H_{ps,1}(z)$ denotes the pseudosensitivity filter, $\nabla_1^{ps}(\ )$ indicates the component of the correlation due to the signal alone, and ω_{res} indicates the frequency of the

[7]Other pseudosensitivity filters are possible that have the required properties for global convergence; however, the other alternatives investigated gave a biased estimate of the signal frequency in the presence of noise.

[8]The work of [12] was based on matching the weighted sum of reference oscillator outputs to the input signal, and it was shown in [33] that this approach was equivalent to a static filter-bank for fixed resonator frequencies. If the resonator frequencies are themselves being adapted, then the weights of the filter have to converge much faster than the resonator frequencies themselves, for the equivalence to hold. Assuming that this is the case, the signal $\mathrm{Im}(Y_m)$ of [12] corresponds to the pseudosensitivity output used in this paper. Hence it would appear that the error signal used to modify the resonator frequencies of this filter-bank structure are very similar to the error signal used to adapt the resonator frequencies of [12]. However, it should be kept in mind that in [12], both the reference frequencies and the weights have to be adapted, and the convergence of the system depends on the weights converging to their steady state much faster than the reference frequencies. These problems are not present in the adaptive system presented here; in fact, there is no need to adapt any weights at all; only the resonator frequencies need be adapted.

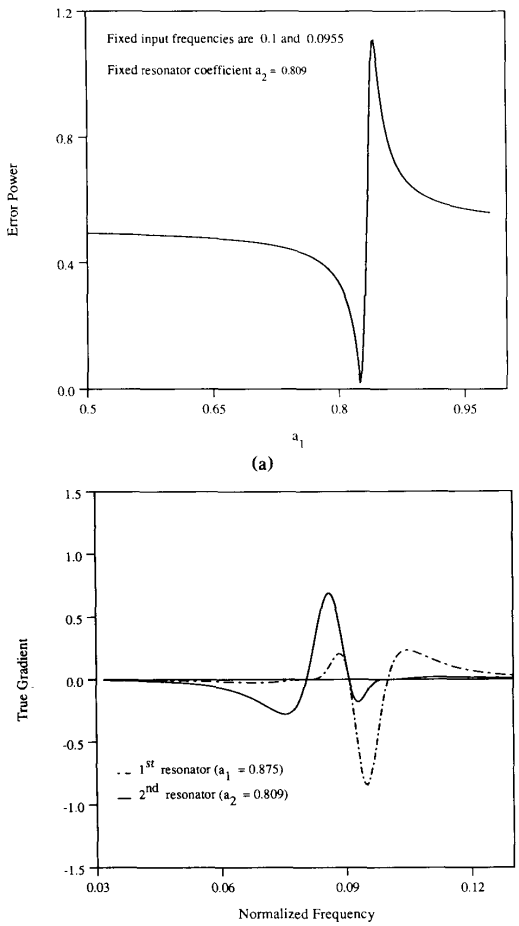

Fig. 4. (a) Error surface for a two-resonator system with input frequencies f_1, f_2, and one resonator frequency (a_2) fixed. (b) True gradient for a two-resonator system with a_1 and a_2 fixed, as a function of the input frequency.

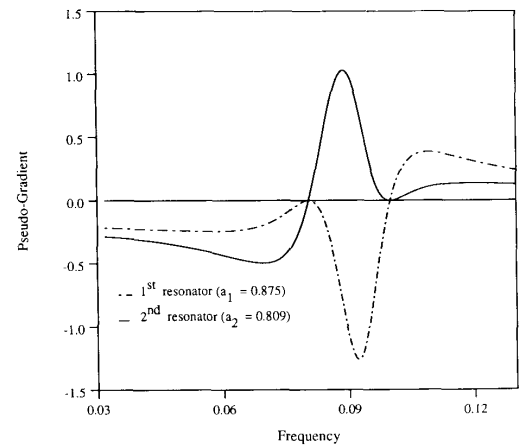

Fig. 5. Pseudogradient for a two-resonator system with a_1 and a_2 fixed.

resonator. (As the resonator is adapting, ∇_1^{ps} becomes a function of the resonator frequency also.) The resonator now adapts until $\nabla(\omega_{in}) = 0$ and finally settles at a frequency ω_1 such that

$$\nabla_1^{ps}(\omega_1, \omega_{in}) = -\frac{2\sigma^2}{2\pi} \operatorname{Re}\left\{\int_0^{\pi} H_e^*(\omega) H_{ps,i}(\omega)\, d\omega\right\}. \tag{27}$$

Hence, the bias in the steady state solution is given by $\omega_{in} - \omega_1$. This bias may be obtained by evaluating the integral in (27) and dividing it by a linear approximation to $\nabla_1^{ps}(\omega)$ near the resonant frequency [11].

By invoking Parsevals theorem in the z domain and the Residue theorem, we can show that

$$\frac{\sigma^2}{2\pi j}\oint H_e(z^{-1}) H_{ps,1}(z) z^{-1}\, dz = 0.$$

Hence, from (27), we have $\nabla_1^{ps}(\omega_1, \omega_{in}) = 0$. This implies that $\omega_1 = \omega_{in}$, i.e., the resonator frequency in the steady state is exactly equal to the input sinusoidal frequency for the case of a single sinusoid. The generalization to the multisinusoidal case is an area of future research.

3.1.3. SNR Enhancement: The SNR enhancement is defined as the ratio of the SNR of the enhanced output to the SNR of the input. As the signal part of the enhanced output is exactly identical to the signal part of the input, the SNR enhancement simply is the ratio of the noise power at the input, to the noise power at the enhanced output. For the single sinusoidal case, the transfer function from the input of the ALE to the enhanced output (the fed back output) is given by $H_{fb,1}(z)$. Therefore, the noise power at the enhanced output, assuming that the input is additive white Gaussian noise, is

$$\overline{n_{enh}^2} = \frac{\sigma^2}{2\pi j}\oint H_{fb,1}(z) H_{fb,1}(z^{-1}) z^{-1}\, dz \tag{28}$$

where σ^2 is the power of the input additive white Gaussian noise. Evaluating the integral for the one-resonator case using the Residue theorem, we obtain

$$\overline{n_{enh}^2} = \frac{\sigma^2 G}{(1-G)} \tag{29}$$

and the SNR enhancement ratio as

$$\text{SNR } enh. = \frac{\sigma^2}{\sigma^2 \dfrac{G}{1-G}} = \frac{1-G}{G}. \tag{30}$$

3.2. Other Applications

The scope of the filter-bank extends to those frequency-domain processing applications that make use of the DFT, and beyond, because of the possibility of having the resonator frequencies arbitrarily placed. In this section, a number of possible applications that use these features are briefly described.

3.2.1. Tracking of Periodic Signals: Many applications deal with the characterization and cancellation of peri-

odic signals. Examples of this include the cancellation of motor noise, noise reduction, and possibly generation of musical tones, and the modal analysis of mechanical structures, to name only a few. In using the filter-bank to deal with such signals, advantage can be taken of the signal periodicity by adapting the frequencies of the resonators while constraining the individual resonators to be harmonically related to the lowest frequency resonator. This constraint allows for much faster convergence, especially when a large number of harmonics are being tracked.

The proposed approach is closely related to the approach of [9], [18], and [20], which use state estimators to obtain the spectral estimates of a periodic signal; however, unlike [20], it does not require the period of the input signal to be known *a priori*. In [9] and [18], the identity observer was originally intended to obtain an N-point DFT of the input samples. This identity observer yields the DFT if its gain vector is constrained so as to provide "deadbeat" behavior[9], and it was shown in [19] to be equivalent to a parallel bank of Nth-order FIR filters. It was suggested in [20] that replacing the FIR filters by IIR filters would improve the reliability of the estimates at the cost of slower convergence of the observer states.[10] This method however, requires the state space modeling of the bandlimited signal to be accurate, i.e., the frequencies of the resonators in the model must be equal to the frequencies of the input signal, else the observer states will never converge to the states of the model. This requires the period of the signal to be known, and the lowest resonator frequency is set equal to the fundamental frequency.

The filter-bank structure of Fig. 1 with the resonator frequencies set equal to the fundamental frequency of the bandlimited signal and its harmonics, is similar to the structure described in [20] with the elements of the observer gain matrix being simply G. However, unlike [20], here the frequency of the fundamental resonator (the resonator with the lowest frequency is called the fundamental resonator) is adapted, with the other resonator frequencies being harmonically related to the fundamental, until it locks on to the fundamental frequency of the quasi-periodic bandlimited signal. Hence, even if the initial model is inaccurate, after the filters converge, the modeling of the signal is accurate.

In the proposed scheme, the fundamental resonator coefficient is adapted using an update that is different from the updates described earlier (to improve the convergence speed). The outputs of all the pseudosensitivity filters (scaled versions of the $x_{q,i}$ of Fig. 1) are summed and then correlated with the error signal, and the resonant frequency of the fundamental resonator is then updated by adapting its coefficients according to the normalized update [10]

$$k_f(n+1) = k_f(n) - \mu \frac{x_e(n) \sum_{i=1}^{i=N} x_{s,i}(n)}{\|x_{s,1}\|^2 + P_{\min}}. \quad (31)$$

Global convergence can no longer be guaranteed in this scheme; however, convergence was obtained for most practical signals, with the fundamental resonator initialized at a frequency greater than the fundamental frequency of the input. At each iteration, the coefficients of all resonators other than the fundamental resonator are set to values that harmonically relate the resonator frequencies to the fundamental resonator frequency.

After the filter has converged, the jth feedback signal ($x_{fb,j}$ in Fig. 1) exactly matches the isolated jth harmonic of the input, in the absence of noise, and under the assumption that the number of resonators is greater than or equal to the number of input signal harmonics. The magnitude and phase of the jth harmonic can be obtained by sampling $x_{fb,j}$ and a 90° phase shifted version of $x_{fb,j}$. As mentioned earlier, these quadrature outputs can be obtained at the $x_{q,j}$ outputs of Fig. 1. If i_j and q_j denote samples of $x_{fb,j}$ and the 90° shifted signal, taken at time t, then the amplitude and phase of the jth harmonic are given by

$$\text{magnitude of } j\text{th frequency component} = \sqrt{i_j^2 + q_j^2} \quad (32)$$

$$\text{phase of } j\text{th frequency component} = \arctan q_j / i_j - \left[(j\omega_f t) \bmod 2\pi\right]. \quad (33)$$

If t is taken as $2\pi n/\omega_f$,[11] then the second term in the expression for the phase goes to zero making the phase computation simpler.

3.2.2. Sub-band Coding: A filter-bank having resonators uniformly placed between dc and half the sampling frequency can be combined with its transpose filter structure [22] to realize a very efficient sub-band coder [23]. The transfer function from the input to the ith output of the analysis-bank is given by

$$G_i(z) = \frac{GH_i(z)}{1 + G\sum_{j=1}^{N} H_j(z)} \quad \text{where} \quad H_i(z) = \frac{z_i z^{-1}}{1 - z_i z^{-1}}$$

and choosing[12] the transfer function from the ith input of the synthesis-bank to its output as $z_i^{-1} z G_i(z)$, the overall transfer function from the input of the analysis-bank to

[9]The identity observer is driven by samples of the input signal and attempts to emulate the states of the model that produced the signal [9], [18]. If the observer is "deadbeat," its states converge to those of the model in N samples. If the original model is observable, appropriate choice of the G matrix ensures this condition.

[10]This is equivalent to setting the G matrix so that the error between the states of the model and the observer take longer than N samples to die to zero. The noise smoothing properties arise because the spectral estimate is made on the basis of more than N samples.

[11]The use of an instantaneous estimate for the gradient causes the coefficient k_f to oscillate about its mean value when the input is noisy. Hence, the sequence $k_f(n)$ is low-pass filtered to get the average value k_{fav}, which is used to calculate the fundamental frequency using $\omega_f = 2\arcsin(k_f/2)$, and hence the sampling times.

[12]This choice of transfer function was motivated by a suggestion from one of the reviewers, in order to make $T(z)$ equal to a perfect delay.

the output of the synthesis-bank is given by

$$T(z) = \sum_{i=1}^{2N} z_i^{-1} z G_i^2(z). \tag{34}$$

By appropriately choosing G, $T(z)$ can be made to equal a scaled delay, which is one of the properties required for a sub-band coder. By grouping the terms arising from the resonators with complex conjugate poles, we can write

$$T(z) = 2G^2 \sum_{i=1}^{N} \left[A_i(z)\left(a_i(1+z^{-2}) - 2z^{-1}\right)\right]\left[A_i(z)z^{-1}\right] \tag{35}$$

where $a_i \pm jb_i = z_i$ are the poles of the first-order resonators, and

$$A_i(z) = \frac{\dfrac{1}{1-2a_i z^{-1} + z^{-2}}}{1 + G\sum_{j=1}^{2N} H_j(z)}. \tag{36}$$

The first term in square brackets in (35) is the desired transfer function from the input to the ith output of the filter-bank filter, and the second term is the desired transfer function from the ith input of the transpose structure to its output.

With the N resonator frequencies uniformly distributed on the unit circle as $\pi/(2N)$, $3\pi/(2N), \cdots$, $(2N-1)\pi/(2N)$, and with G set equal to $1/2N$, the transfer function $T(z)$ is given by (Appendix A.3)

$$T(z) = 2NG^2 z^{-2N}. \tag{37}$$

Besides being very efficient to implement, the proposed sub-band coder has the desired feature that the number of sub-bands need not be a power of 2.

It is also conjectured that a frequency-division multiplexed system could be realized by interchanging the order of the filter-bank filter and the transpose filter. In both applications, it is possible that smaller side-lobes and steeper transition regions could be achieved by grouping a number of resonators into single channels [4].

3.2.3. Frequency-Domain Adaptive Filtering: In frequency-domain filtering, filters are usually used to separate the input signal and the desired signal into narrow-band signals and the adaptation is then performed to match the narrow-band subcomponents. Now, by taking the filter-bank outputs to be something other than $x_{fb,i}$ (as explained later in Section IV), but with the feedback signals still being $x_{fb,i}$, it is possible to make the filter-bank outputs add up to exactly unity, for any set of resonator frequencies. By making use of this fact, it is possible to eliminate the inverse filter that is typically needed to recombine the sub-bands into a single desired signal. Also, by adapting narrow-band signals, the convergence time can often be much smaller. A typical example of a frequency-domain noise canceller based on the filter-bank is shown in Fig. 6. An adaptive master filter-bank is used to divide the noise signal $n(t)$ into narrow-band signals $n_i(t)$. An identical slave filter-bank is used to divide the signal $x_{in}(t)$ plus filtered noise $n'(t)$ into sub-bands. Weighted sums in the in-phase and quadrature components of the narrow-band noise signals are then individually adapted to minimize the narrow-band signals $e_1, e_2, \cdots, e_N$, and hence cancel the noise component $n'(t)$. By using an adaptive master filter-bank, a number of benefits can be accrued. Firstly, the adaptation is largely unaffected by large signal components at frequencies where no noise exists. Secondly, the number of resonators required is reduced when the noise is composed of narrow-band components only.

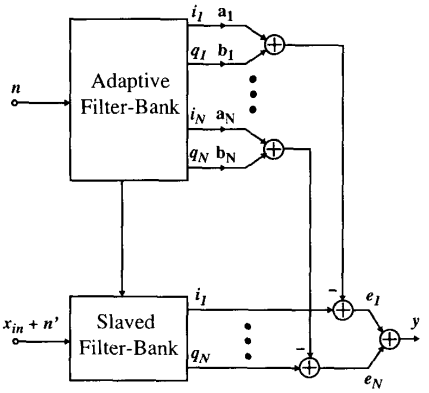

Fig. 6. Block diagram of frequency-domain noise canceller.

A very similar scheme can be used to adapt a signal to a desired signal. In this case, the signal is input to the master-filter, and the desired signal is input to the slave-filter, and the output is taken as the sum of the narrow-band outputs of the master-filter (i.e., the sum of the x_i signals in Fig. 6).

3.2.4. Multi-Narrow-band Phased-Arrays: The use of phased-array sensors in applications such as sonar and radar detection, seismic analysis, microwave imaging, etc., has become widespread. Many of the most powerful processing algorithms for signals detected by sensor arrays are based on the assumption that the signals are narrow-band [24, ch. 14]. For many applications, these algorithms cannot be used because multi-narrow-band signals are present due to reasons such as multiple sources, Doppler shifted reflections, layers of different propagation media, etc. The system shown in Fig. 7 would allow the decomposition of these signals into isolated narrow-band signals.

In this approach, a master filter-bank is used to adapt to the spectral peaks of the average output of all the sensors. The individual outputs of each sensor are then filtered into narrow-band in-phase and quadrature subcomponents by slaved filter-banks. Each of these sub-bands could then be individually processed using narrow-band techniques. For example, it is possible to control the directivity of each sub-band independently, and to individually adapt the sub-bands to eliminate errors due to nonuniform spacing of the sensors. Also, by adaptively

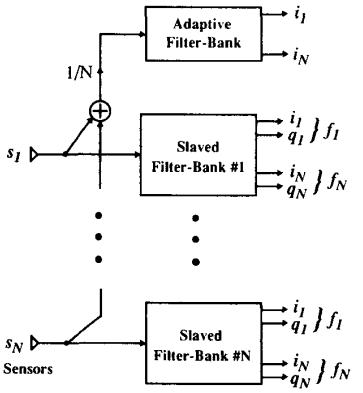

Fig. 7. Block diagram for phased array applications.

subtracting the differences between the sub-band outputs of adjacent sensors, super-resolution can be achieved similar to the Griffiths–Jim approach of fig. 14.27 in [24]. The practicality of this approach is strongly dependent on the complexity of the filter-bank filters due to the large number of required filters. It is feasible that each slave-filter could be implemented by a single DSP chip with sampling rates as high as 100 kHz at the present time. Alternatively, it is conceivable that the slave-filters could be implemented at much higher frequencies using analog circuits. This is an interesting area for future research.

IV. The Special Case of LDI-Based Resonators

So far, the derived properties and applications of the filter-bank hold for the general case, where any biquad structure (subject to the constraints (13) for the line enhancer case) may be used to implement the transfer function (5) of the resonators. In this section, we will specifically choose the LDI-based biquad to replace the resonators of Fig. 1. These biquads provide hardware efficient structures that have good sensitivity properties, especially for low resonant frequencies, and also good noise properties, as explained below. Alternatively, other biquad structures could also be used, or resonators with different resonant frequencies could be implemented with different biquad structures, that have good properties (sensitivity, noise, complexity, etc.) for that frequency range.

It was shown in [1] that if the resonators are implemented as complex first-order resonators, or if a pair of resonators with complex conjugate poles are implemented using second-order sections [1], [27], [28] that preserve the internal orthogonality of the system state variables, then the filter structure has several nice properties, such as minimum roundoff noise, no zero input limit cycles, etc. [29], [30]. In order to preserve the orthogonality of the internal states (for a white noise input), a set of sufficient conditions can be derived for the state space representation of the second-order sections (summarized in Appendix A.1). Unfortunately, the LDI resonators used in this paper do not satisfy these conditions. Hence, the nice properties mentioned in [1] are not necessarily true. However, for the case where the resonator pole frequencies are low valued, the LDI resonators almost satisfy these conditions (see Appendix A.2); in such cases, if the damping factor G is chosen as $1/2N$, it is conjectured that the filter structure will exhibit the good properties described in [1].

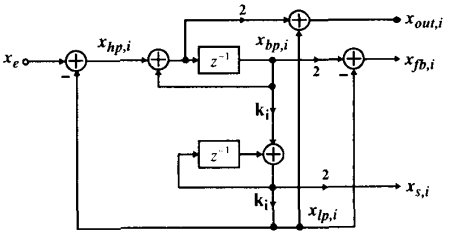

Fig. 8. Single resonator of filter-bank structure based on constant bandwidth LDI biquad.

The LDI resonators also possess the advantage of requiring only two multipliers, as compared to the four multiplier structures of [1], [27], [28].[13] Also, as shown in Appendix A.2, for low valued resonant frequencies, the pole positions of the LDI resonators are not very sensitive to coefficient truncation. Further, coefficient truncation only causes the angular position of the poles to change, but still retains them on the unit circle. This property of the LDI resonators causes the overall transfer function to be insensitive to the filter coefficients, for frequencies in the vicinity of the resonator pole frequencies [31].

The desired transfer function (5) can be realized by the constant bandwidth LDI biquad shown in Fig. 8, where the common feedback term is denoted $x_{fb,i}$, and the quadrature output $x_{q,i}$ can be obtained by multiplying $x_{s,i}$ by $\cos(\omega_i T/2)$. The overall filter-bank is shown in Fig. 9. The internal coefficient k_i of the biquads is related to their $a_i(=\cos(\omega_i T)$ through the relation (6), and the conditions to ensure the stability of the filter-bank (10) become

$$G < \frac{1}{N} \quad \text{and} \quad 0 < k_i < 2. \tag{38}$$

Also, the expression da_i/dk_i in (26) now becomes $-2k_i$, which is seen to be negative for all possible values of k_i, as required by (13).

The pseudosensitivity output for this application may be obtained as the $x_{s,i}$ shown in Fig. 9. As far as the sub-band coder is concerned, the outputs of the analysis-

[13]It was pointed out by one of the reviewers that it is possible to derive a one multiplier second-order section [34], by applying a diagonal similarity transformation on the "internally orthogonal" structure of [1]. This is a possible area for future research.

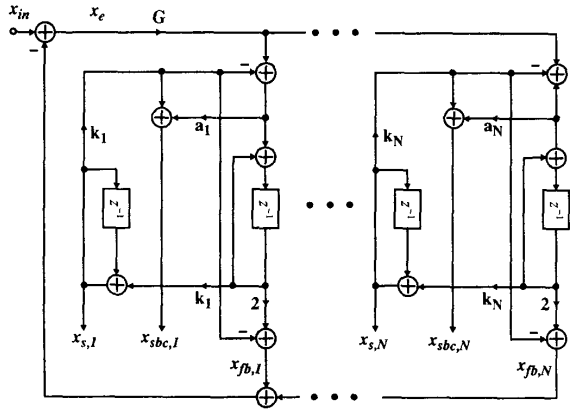

Fig. 9. LDI-based filter-bank structure.

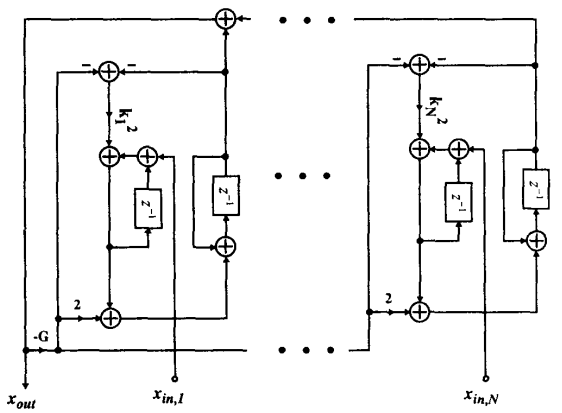

Fig. 10. Signal flow graph of transpose structure used in sub-band coding.

bank may be obtained as $x_{sbc,i}$ of Fig. 9, and the synthesis-bank may be implemented using the transpose of a structure similar to the analysis-bank, as shown in Fig. 10. Unfortunately, because of the use of the coefficient k_i^2 instead of k_i in the synthesis-bank, this structure is not very well scaled; however, it is conjectured that the use of other biquad structures could result in a better scaled synthesis-bank.

Alternatively, if the resonator outputs are taken as $x_{out,i}$ in Fig. 8, but with the feedback signal still being $x_{fb,i}$, and the damping G is taken as $1/2N$, then it is easily shown [2], [4] that the sum of all the outputs is equal to unity independent of the resonant frequencies of the biquads. As mentioned in Section 3.2.3, this property can be important in some applications. There are many other possibilities for LDI-based resonators that also result in a property that the sum of the outputs of the resonators is exactly unity. For example, Fig. 11 shows a possible realization of a constant-Q resonator possessing this property.

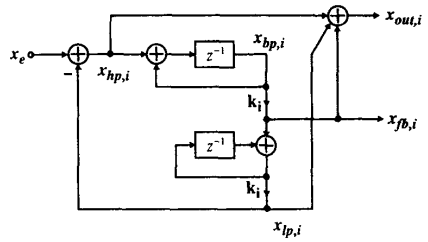

Fig. 11. Single resonator of filter-bank structure based on constant Q LDI biquad.

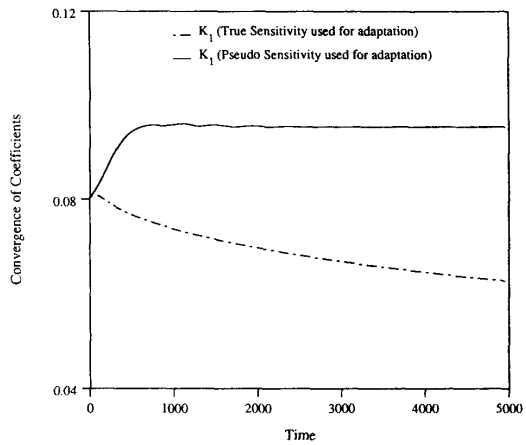

Fig. 12. Convergence of coefficients of two-resonator system for true and pseudogradient updates with one resonator fixed.

V. Simulations of the LDI-Based Filter-Bank

5.1. Comparison of Performance of True and Pseudogradients

Simulations of the performance of a two-resonator system, when the true-sensitivity and pseudosensitivity filters are used, are shown in Fig. 12. The simulated system consists of two resonators, one with a resonant frequency of 0.1 which is fixed, and with the other resonator adapting to notch out an input sinusoid at a frequency of 0.09545. A μ value of 0.0001 is used to adapt both resonators, and the damping factor G is set equal to $1/12$. It can be seen that when the true sensitivities are used, convergence is not obtained.

5.2. Bias in Resonator Frequency

To confirm the derivations made in Section 3.1.2, a plot of the percentage bias in the resonator frequency as obtained from simulations is compared to the theoretical value of zero in Fig. 13, for an input SNR of 10 dB and 0 dB for $G = 1/6$. The simulated system consists of a single resonator in a feedback loop, and the coefficient k_1 of the resonator is adapted using an instantaneous approxi-

mation to the gradient as

$$k_1(n+1) = k_1(n) - \mu e(n) s_1(n)$$

where $e(n)$ is the error and $s_1(n)$ is the pseudosensitivity output. The bias shown in the simulations is seen to be negligibly small, which is in accordance with the theory. This condition of zero bias is valid only for the case of one resonator tracking a single input frequency; for multiple resonators, a bias is expected to exist but as of date, it has not been possible to derive theoretical expressions for this general case.

5.3. Simulations of the Line Enhancer

Simulations of the performance of the adaptive line enhancer are shown next. The resonator coefficients are adapted using the power normalized update [13]

$$k_i(n+1) = k_i(n) - \mu \frac{s_i(n) e(n)}{\|s_i\|^2 + P_{\min}}$$

where $s_i(n)$ is the ith pseudosensitivity output and $e(n)$ is the error output. Here, an instantaneous approximation has been used for the pseudogradient, and the power normalization is done in order to speed up convergence when the resonator coefficients are far away from their steady-state values.

For the simulations presented, G is set equal to $1/12N$, where N is the number of resonators, $P_{\min}$ is set equal to 0.002, and to prevent the tracking of resonators from being identical, the μ value of the different resonators is separated from each other by 10% of the largest μ value. Also, the input signal is normalized so as to have unit power.

The first example (see Fig. 14(a)) shows the convergence of the coefficients of a system of three resonators, with the resonator frequencies initialized at 0.08, 0.10, and 0.12, and the input being the sum of three sinusoids in white noise, with frequencies 0.1, 0.12, and 0.14, respectively, all with an SNR of 10 dB. A μ value of 0.001[14] is used for the first resonator.

The second example (see Fig. 14(b)) shows convergence when the resonator frequencies are initialized far away from the steady-state values. The input consists of two sinusoids with frequencies 0.125 and 0.13 with an SNR of 3 dB each. The resonator frequencies were initialized at 0.001 and 0.002, respectively, and a μ value of 0.0001 is used for the first resonator.

The third example (see Fig. 14(c)) shows convergence when a two-resonator system tracks two input sinusoids with different powers. The resonator frequencies are initialized at 0.1 and 0.11, and the input consists of two sinusoids with frequencies 0.12 and 0.14 at an SNR of 20 dB and 0 dB, respectively. This simulation used a μ value of 0.001 for the first resonator.

[14] In the examples presented, the μ value was chosen arbitrarily. However, for the one-resonator case, it is possible to interpret the tracking loop as a phase-locked-loop, with a second-order loop filter. This should enable the μ to be chosen so as to obtain any desired transient response. This idea was used in a recently presented paper [35]. However, as the generalization for the multiple resonator case is not straightforward, it is not clear at this time how the μ values can be chosen in a systematic fashion to get a desired transient response.

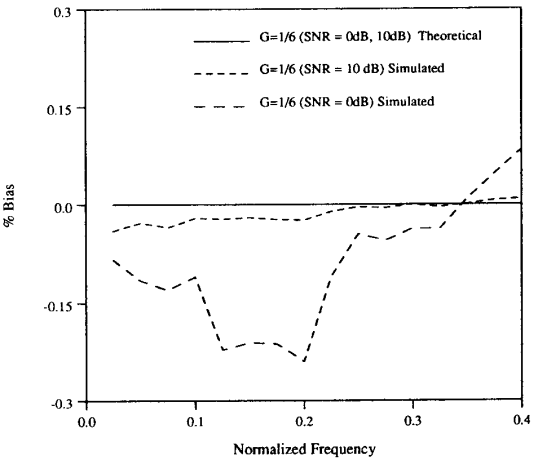

Fig. 13. Bias plot for one-resonator system.

5.4. Tracking of Periodic Signals

A simulation of a four-resonator system tracking a periodic input signal is shown next in Fig. 15. The input signal has four components with frequencies 0.02, 0.04, 0.06, and 0.08, with the amplitude and initial phase of these components being (0.5,0), (1.0,0.3), (0.25,0.9), and (0.33,1.8), respectively, with the noise power of the input such that the frequency component at 0.06 has an SNR of 10 dB. The fundamental resonator frequency is initialized at 0.025 and the other resonator frequencies are forced to be harmonically related to this fundamental resonator frequency. The enhanced outputs $x_{fb,i}$ and their 90° shifted versions are sampled at times $t = 2\pi n/\omega_f$ and the amplitude and phase of the different frequency-components are obtained from these samples.

VI. Conclusion

A resonator-based filter-bank was proposed, based on a modification of the LDI simulation of a singly terminated ladder filter. Some properties and applications of the generalized filter-bank were examined, and it was shown to be an excellent choice for spectral line enhancement, due to its simplicity, output signal orthogonality with sinusoidal inputs, low bias, and good convergence properties. A number of additional possible applications were also briefly described. A specific implementation of the filter-bank was next examined, which is very hardware efficient, and low-noise for low-resonator pole frequencies, because of the use of LDI-based resonators. Finally, a number of computer simulations were presented for the LDI-based filter-bank to substantiate the theoretical derivations of the earlier sections. Many of the simulations showed excellent behavior even for low SNR's and

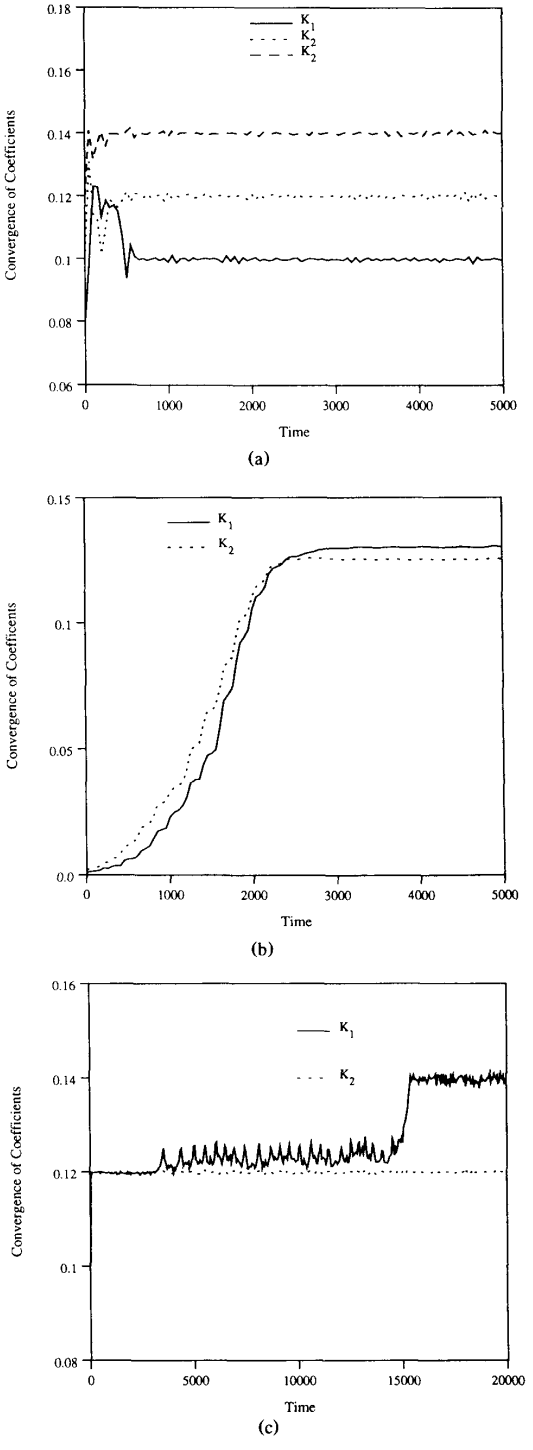

Fig. 14. (a) Convergence of the coefficients of a three-resonator system. (b) Convergence of the coefficients of a two-resonator system. (c) Convergence of the coefficients of a two-resonator system for input frequency components with different powers.

closely spaced sinusoids, sometimes with the sinusoids having very different power levels.

A. Appendix

A.1. Sufficient Conditions for Preservation of Good Properties of the Filter Structure

We will consider the filter structure of Fig. 1, with the resonators being second-order sections, and derive sufficient conditions for the filter structure to have the nice properties mentioned in [1]. It should be noted that these conditions were implied in [1], and the main motivation for stating them explicitly here is to show that under certain circumstances, the LDI resonators almost satisfy these properties. Let the state-space description of the single input single output second-order sections of Fig. 1 be

$$X(n+1) = AX(n) + bu(n)$$
$$y(n) = cX(n) + du(n).$$

Following on the lines of [1], the state-space description of the overall system may be developed easily, and these results will not be repeated here. Now, the minimum roundoff noise condition requires that the observability and controllability grammian (denoted W and K in [1]) be diagonal positive definite matrices (which is equivalent to saying that the system states are orthogonal for white noise input [29]). Further, this condition also automatically ensures that the filter structure is limit cycle free. It can be shown that these conditions are satisfied if the scale factor is properly chosen, and the following condition holds true for the second-order sections:

$$A^TA = I,\ cc^T = p,\ b = Ac^T,\ d = 0,$$
$$\text{where } p \text{ is some scalar.} \quad \text{(A.1.1)}$$

These conditions are seen to be satisfied by the second-order section of [1], the coupled form [27], and some of its modifications [28].

A.2. Properties of LDI Resonators

The sensitivity properties of the LDI based resonators are briefly derived. It is also shown that they are almost "internally orthogonal" for low values of the resonant frequencies. The transfer function of an all-pole LDI biquad is

$$H_{ldi}(z) = \frac{z^{-2}}{1-(2-k_i^2)z^{-1}+z^{-2}} \quad \text{(A.2.2)}$$

and the pole radius and angle are given by the expressions

$$r = 1 \quad \text{and} \quad \theta_i = 2\operatorname{asin}(k_i/2). \quad \text{(A.2.3)}$$

Hence the sensitivities are given as

$$S_{k_i}^r = \frac{\partial r}{\partial k_i} = 0 \quad \text{and} \quad S_{k_i}^{\theta_i} = \frac{\partial \theta_i}{\partial k_i} = \frac{1}{\sqrt{1-k_i^2/4}}. \quad \text{(A.2.4)}$$

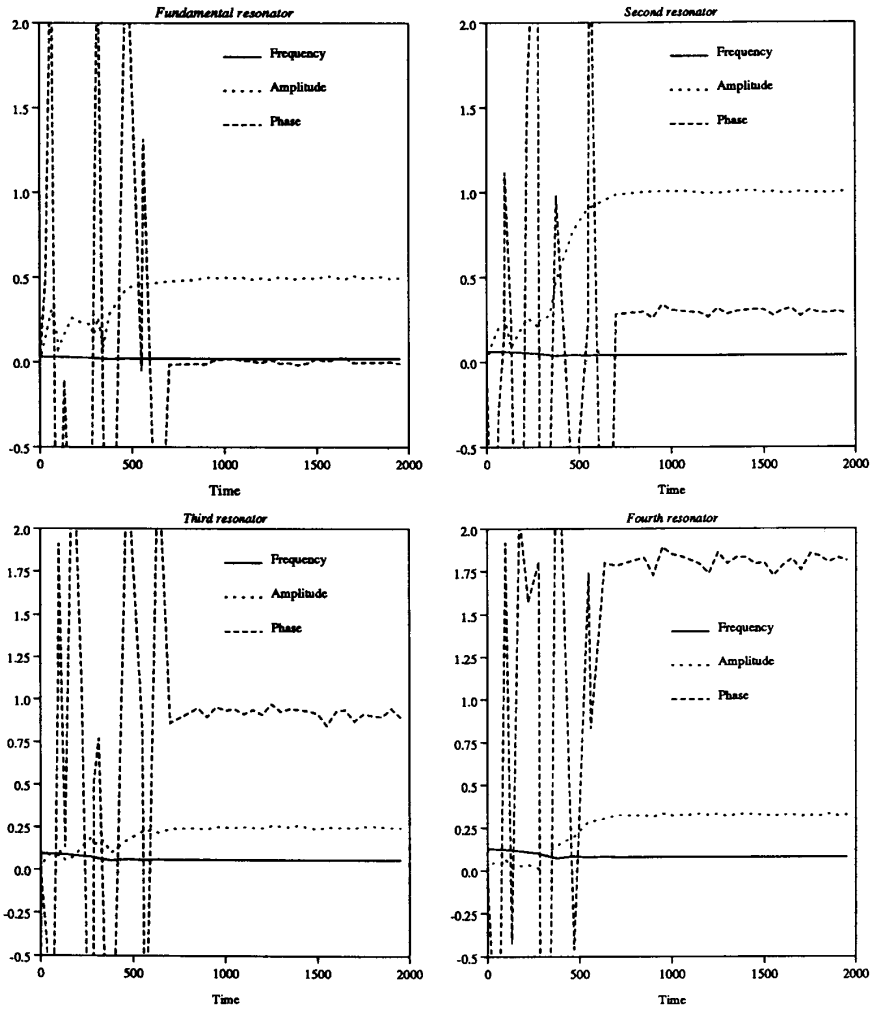

Fig. 15. Tracking of a periodic signal.

It may be seen that the poles are always on the unit circle, and the sensitivity of the pole angle to the k_i is least when k_i is small.

We will now develop the state-space description of the resonator. With reference to Fig. 3(a), if $x_{1,i}$ is labelled as the state variable x_1, and the output of the other delay element is taken as the second state variable x_2, then the state-space description of the system is

$$\begin{bmatrix} x_1(n+1) \\ x_2(n+1) \end{bmatrix} = \begin{bmatrix} 1-k_i^2 & -k_i \\ k_i & 1 \end{bmatrix} \begin{bmatrix} x_1(n) \\ x_2(n) \end{bmatrix} + \begin{bmatrix} 1 \\ 0 \end{bmatrix} x_e(n) \tag{A.2.5}$$

$$y(n) = \begin{bmatrix} 2-k_i^2 & -k_i \end{bmatrix} \begin{bmatrix} 1 \\ 0 \end{bmatrix}. \tag{A.2.6}$$

For low values of k_i, it may be seen that the conditions (A.1.2) are almost satisfied.

A.3. Derivation of Sub-band Coder Transfer Function

For z_i chosen as $e^{j2\pi(i+0.5)/2N}$ and $G = 1/2N$, recognizing the fact that $z_i^{2N} = -1$, the expression for $H_i(z)$ as defined in Section 3.2.2 may be rewritten as

$$H_i(z) = \frac{1}{1+z^{-2N}} \left[z_i z^{-1} + \cdots + z_i^{2N} z^{-2N} \right]. \tag{A.3.7}$$

Hence the loop gain $G\Sigma_{i=1}^{2N} H_i(z)$ may be derived to be simply $-z^{-2N}/1+z^{-2N}$, and consequently, the transfer function $G_i(z)$ may be derived to be

$$G_i(z) = G\left[z_i z^{-1} + \cdots + z_i^{2N} z^{-2N} \right]. \tag{A.3.8}$$

Now, we are interested in deriving an expression for $\Sigma_{i=1}^{2N} G_i^2(z)$. Using the expression (A.3.8) for $G_i(z)$, and noting the fact that

$$\sum_{i=1}^{2N} z_i^k = \begin{Bmatrix} -2N, & k = 2N \\ 2N, & k = 4N \\ 0, & \text{otherwise} \end{Bmatrix} \tag{A.3.9}$$

the transfer function $T(z)$ can be shown to be

$$T(z) = 2NG^2 z^{-2N}. \qquad \text{(A.3.10)}$$

Acknowledgment

The authors are most grateful to Prof. W. F. McGee for several useful discussions, and to Prof. Gabor Peceli and the anonymous reviewers for their careful perusal of the manuscript and their constructive suggestions.

References

[1] G. Peceli, "Resonator based digital filters," *IEEE Trans. Circuits Syst.*, vol. CAS-36, pp. 156–159, Jan. 1989.
[2] ___, "Structurally passive resonator based digital filters," in *Proc. Int. Symp. Circuits and Systems*, 1988.
[3] W. F. McGree, "Frequency interpolation filter bank," in *Proc. Int. Symp. Circuits and Systems*, pp. 1563–1566, 1989.
[4] ___, "Fundamental relations between LMS spectrum analyzer and recursive least squares estimation," *IEEE Trans. Circuits Syst.*, vol. CAS-36, pp. 151–153, Jan. 1989.
[5] ___, Univ. Ottawa, correspondence, Sept. 1989.
[6] J. T. Lim, private conversation, Bell Northern Research, Ottawa, 1977.
[7] B. Widrow *et al.*, "Fundamental relations between the LMS algorithm and the DFT," *IEEE Trans. Circuits Syst.*, vol. CAS-34, pp. 814–820, July 1987.
[8] J. R. Glover, Jr., "Adaptive noise cancelling applied to sinusoidal interferences," *IEEE Trans. Acoust., Speech, Signal Processing*, vol. ASSP-25, pp. 484–491, Dec. 1977.
[9] G. H. Hostetter, "Recursive discrete Fourier transformation," *IEEE Trans. Acoust., Speech, Signal Processing*, vol. ASSP-28, pp. 184–190, Apr. 1980.
[10] K. Martin and M.-T. Sun, "Adaptive filters suitable for real-time spectral analysis," *IEEE Trans. Circuits Syst.*, vol. CAS-33, pp. 218–229, Feb. 1986.
[11] T. Kwan and K. Martin, "Adaptive detection and enhancement of multiple sinusoids using a cascade IIR filter," *IEEE Trans. Circuits Syst.*, vol. CAS-36, pp. 937–946, July 1989.
[12] A. Ogunfunmi and A. Peterson, "Adaptive methods for estimating amplitudes and frequencies of narrowband signals," in *Proc. Int. Symp. Circuits and Syst.*, pp. 2124–2127, 1989.
[13] K. W. Martin, "Power normalized update algorithm for adaptive filters without divisions", *IEEE Trans. Acoust., Speech, Signal Processing*, vol. 37, pp. 1782–1786, Nov. 1989.
[14] ___, "The isolation of undistorted sinusoids in real-time," *IEEE Trans. Circuits Syst.*, vol. 38, pp. 360–364, Feb. 1990.
[15] D. Hush, N. Ahmed, R. David, and S. D. Stearns, "An adaptive IIR structure for sinusoidal enhancement, frequency estimation, and detection," *IEEE Trans. Acoust., Speech, Signal Processing*, vol. ASSP-34, pp. 1380–1390, Dec. 1986.
[16] D. V. B. Rao and S. Y. Kung, "Adaptive notch filtering for the retrieval of sinusoids in noise," *IEEE Trans. Acoust., Speech, Signal Processing*, vol. ASSP-32, pp. 791–802, Aug. 1984.
[17] A. Nehorai, "A minimal parameter adaptive notch filter with constrained poles and zeros," *IEEE Trans. Acoust., Speech, Signal Processing*, vol. ASSP-33, pp. 983–996, Aug. 1985.
[18] G. Peceli, "A common structure for recursive discrete transforms," *IEEE Trans. Circuits Syst.*, vol. CAS-33, pp. 1035–1036, Oct. 1986.
[19] R. R. Bitmead, "On recursive discrete Fourier transformation," *IEEE Trans. Acoust., Speech, Signal Processing*, vol. ASSP-30, pp. 319–322, Apr. 1982.
[20] R. R. Bitmead *et al.*, "A Kalman filtering approach to short-time Fourier analysis," *IEEE Trans. Acoust., Speech, Signal Processing*, vol. ASSP-34, pp. 1493–1501, Dec. 1986.
[21] S. Haykin, *Adaptive Filter Theory*. Englewood Cliffs, NJ: Prentice Hall, 1986.
[22] A. V. Oppenheim and R. W. Schafer, *Digital Signal Processing*. Englewood Cliffs, NJ: Prentice Hall, 1975.
[23] N. S. Jayant and P. Noll, *Digital Coding of Waveforms*. Englewood Cliffs, NJ: Prentice Hall, 1984.
[24] B. Widrow and S. D. Stearns, *Adaptive Signal Processing*. Englewood Cliffs, NJ: Prentice Hall, 1975.
[25] L. T. Bruton, "Low-sensitivity digital ladder filters," *IEEE Trans. Circuits Syst.*, vol. CAS-24, pp. 567–571, Sept. 1977.
[26] R. Gregorian and G. C. Temes, *Analog MOS Integrated Circuits for Signal Processing*. New York: Wiley, 1986.
[27] J. Szczupak and S. K. Mitra, "On digital filter structures with low coefficient sensitivities," *Proc. IEEE*, vol. 66, pp. 1082–1084, Sept. 1978.
[28] G.-T. Yan and S. K. Mitra, "Modified coupled-form digital-filter structures," *Proc. IEEE*, vol. 70, pp. 762–763, July 1982.
[29] C. T. Mullis and R. A. Roberts, "Synthesis of minimum roundoff noise fixed point digital filters," *IEEE Trans. Circuits Syst.*, vol. CAS-23, pp. 551–562, Sept. 1976.
[30] P. P. Vaidyanathan and V. Liu, "An improved sufficient condition for absence of limit cycles in digital filters," *IEEE Trans. Circuits Syst.*, vol. CAS-34, pp. 319–322, Mar. 1987.
[31] G. Pecili, "Sensitivity properties of resonator-based digital filters," *IEEE Trans. Circuits Syst.*, vol. CAS-35, pp. 1195–1197, Sept. 1988.
[32] M. E. Van Valkenburg, "*Introduction to Modern Network Synthesis*. New York: Wiley, 1960.
[33] W. F. McGee and G. Zhang, "Logarithmic filter banks," in *Proc. Int. Symp. Circuits and Systems*, pp. 661–664, 1990.
[34] A. Fettweis, "Passivity and losslessness in digital filtering," *AEU*, pp. 1–8, Jan./Feb. 1988.
[35] T. Kwan and K. Martin, "A notch-filter-based frequency-difference detector and its applications," in *Proc. Int. Symp. Circuits and Systems*, pp. 1343–1346, 1990.

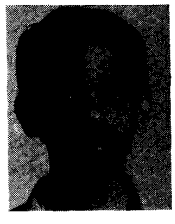

Mukund Padmanabhan (S'87) received the B. Tech. (Hons.) and the M.S.E.E. degree from the Indian Institute of Technology, Kharagpur in 1987, and the University of California, Los Angeles in 1989, respectively. At present, he is working towards the Ph.D. degree at UCLA.

His research interests are in signal processing, digital and analog filters, and analog integrated circuits.

Kenneth Martin (S'75–M'80–SM'89–F'91) received the B.A.Sc. (graduating at the top of his class) and the M.A.Sc. from the University of Toronto, Canada in 1975 and 1977, respectively. He obtained a Ph.D. in 1980.

Since then he has been employed by the Electrical Engineering Department at UCLA where he presently is a Full Professor. He has also been a consultant to many high technology companies including Xerox Corp., Hughes Aircraft Co., Intel Corp., and BrookTree Corp. in the areas of high-speed analog and digital integrated circuit design. He has ongoing research programs in the areas of analog CMOS systems, high-speed GaAs MESFET and HBT circuits, and digital-signal-processing algorithms for fixed and adaptive filters.

Professor Martin served as an Associate Editor of the Transactions on Circuits and Systems from 1985 to 1987, and has served on the technical committee for many International Symposia on Circuits and Systems. He was awarded a National Science Foundation Presidential Young Investigator Award that ran from 1985 to 1990.